Predicting Fatigue Life of Composite Wind Turbine Blades Using Constituent-Level Physics and Realistic Aerodynamic Loads

Faisal Hasan Bhuiyan[1], Dimitri J. Mavriplis [2] and Ray S. Fertig, III [3]
University of Wyoming, Laramie, WY, 82071

Use of composite materials is widespread in the wind industry. The design life of a wind turbine blade is typically 20 years and its oscillatory nature requires it to perform under cyclic loading. Thus, fatigue life prediction of wind turbine blades is an important part of blade design. In this paper, we present a comprehensive physics-based methodology for predicting fatigue life of a realistic composite wind turbine blade, working under realistic aerodynamic loads generated using a CFD model. The wind turbine blade has been modeled using blade data released by the Sandia National Labs. Aerodynamic loads on the blade are computed using an in-house aeroelastic coupling to the CFD code NSU3D. A physics-based material model for fatigue based on the kinetic theory of fracture is incorporated in the structural model to predict structural-level composite fatigue life.

Nomenclature

B_i	=	static failure coefficients of the matrix failure criterion
$\boldsymbol{C}_c$	=	composite stiffness matrix (6x6)
$\boldsymbol{C}_f$	=	fiber stiffness matrix (6x6)
$\boldsymbol{C}_m$	=	matrix stiffness matrix (6x6)
h	=	Plank's constant
$\boldsymbol{I}$	=	identity matrix
I_t	=	transversely isotropic matrix stress invariant corresponding to maximum matrix stress normal to the fiber
I_{s1}	=	transversely isotropic matrix stress invariant corresponding to in-plane matrix shear
I_{s1}	=	transversely isotropic matrix stress invariant corresponding to out-of-plane matrix shear
k	=	Boltzmann constant
K_b	=	rate of microcrack accumulation and coalescence
n	=	fatigue damage variable
n_0	=	equilibrium parameter that depends on the damage accumulation exponent
R	=	fatigue load ratio
R_P	=	ratio of two principal composite stresses
T	=	temperature driving the damage accumulation process
U	=	activation energy associated with microcrack accumulation and coalescence
β	=	pressure strengthening coefficient
γ	=	activation volume associated with microcrack accumulation and coalescence
Δt	=	change in time over a particular segment of a load-history curve
$\Delta\sigma_a$	=	change in stress over a particular segment of a load-history curve
$\boldsymbol{\eta_c}$	=	vector describing the coefficient of thermal expansion (CTE) of the composite
$\boldsymbol{\eta_f}$	=	vector describing the CTE of the fiber
$\boldsymbol{\eta_m}$	=	vector describing the CTE of the matrix
λ	=	damage accumulation exponent

[1] PhD student, Department of Mechanical Engineering, 1000 E. University Avenue, Dept. 3295, AIAA Student Member
[2] Professor, Department of Mechanical Engineering, 1000 E. University Avenue, Dept. 3295, AIAA Associate Fellow
[3] Assistant Professor, Department of Mechanical Engineering, 1000 E. University Avenue, Dept. 3295, AIAA Member

$\boldsymbol{\sigma}_c$ = volume average composite stress tensor
$\boldsymbol{\sigma}_f$ = volume average fiber stress tensor
$\boldsymbol{\sigma}_m$ = volume average matrix stress tensor
τ_0 = bulk matrix shear strength
ϕ_f = fiber volume fraction
ϕ_m = matrix volume fraction

I. Introduction

ONE of the major challenges the wind industry faces is the production of electricity at costs competitive with traditional fossil fuel-based electricity production. One significant cost driver is maintenance and repair cost of the blades[1], which are increasingly manufactured using fiber reinforced composites. This cost is to be expected since the typical wind turbine blade is designed to last for 20 years running full-time, which is equivalent to nearly nine times the service life of a commercial aircraft, with an hourly fatigue 48 times greater.[2] Yet in order to keep costs down the typical turbine blade receives only 1.3% of the maintenance time that is afforded a commercial aircraft. This shortage of maintenance causes greater number of blade failures, shorter blade life, and a reduction in aerodynamic performance. To enhance design of turbine blades for longer fatigue life, an improvement in the prediction of fatigue life is necessary.

Wind turbine blades are typically made of fiber-reinforced polymer-matrix composites. For this class of materials, fatigue failure is primarily a matrix-dominated event. Even though fatigue of composite materials has been studied extensively[3, 4], a generalized method to predict the fatigue life of composites has yet to be formulated. Most fatigue prediction methods for composites pertain to a specific load history at a specified temperature and require a great deal of characterization data. Such empirical relationship based models are not well-suited to predict fatigue in a composite structure as large as a wind turbine blade, with the associated variability in loading and operating temperature. Therefore, an appropriate constituent-level physics-based methodology is essential for predicting the fatigue life of a wind turbine blade. Such a methodology for predicting the fatigue life of large composite structures using constituent-level physics has been described by Fertig et al.[5-7] In this methodology, composite fatigue is modeled as a matrix-specific phenomenon using matrix specific physics and it is implemented in three separate modeling steps: (1) a multiscale modeling methodology to link composite stresses and strains to matrix stresses and strains, (2) a physics-based model for fatigue of the matrix material, and (3) a link between the microscopic bond breaking in matrix and the macroscopic fatigue failure of the model. This theory is easily programmable, computationally efficient and the requirement for material characterization data is minimal - which makes it a suitable model to use for fatigue life prediction of large composite structures. Furthermore, it has been previously shown that this multi-scale approach enables the prediction of laminate level fatigue life and failure modes from lamina level characterization data.[6]

As a first component of this analysis, a finite element model (FEM) of a wind turbine blade was constructed. The wind turbine blade model data were gathered from the data released by the Sandia National Labs (SNL). The model of a 13-meter wind turbine rotor used in the Scaled Wind Farm Technology (SWiFT) turbines[8] was used as a basis for this study. Realistic aerodynamic loads were defined on the wind turbine blade using the CFD code NSU3D.[9] Gravity and centrifugal force were also applied on the blade to simulate the operating environment of a typical wind turbine blade. All of these steps provided the necessary platform for the fatigue model to operate upon. This computationally efficient multiscale physics-based fatigue model predict the mean fatigue life of a composite wind turbine blade in addition to prediction of damage initiation and propagation in the blade.

II. Modeling Approach

Three separate modeling efforts were required in our approach to investigating the fatigue life of a wind turbine blade: a realistic finite element (FE) structural model of the wind turbine blade, a computational fluid dynamics (CFD) model to compute realistic aerodynamic loads on the blade, and a physics-based fatigue model for predicting fatigue life of the composite blade. These modeling steps are described in details in the subsequent sections.

A. Structural Model of the Wind Turbine Blade

Realistic structural models are essential to perform realistic fatigue or other structural analysis of a wind turbine blade. Consequently, a finite element model of a composite wind turbine blade has been developed as a basis for the fatigue life investigation. Blade model data from manufacturers is not available due to proprietary reasons. However, the Wind Energy Technologies Department of the Sandia National Laboratories (SNL) has published some model data. One of the few blade models released by SNL is a 100 m 13.2 MW horizontal axis wind turbine (HAWT) blade.[10,

[11] Another blade model available from SNL is the SWiFT turbine aeroelastic model.[8] It is a 13 m blade and currently being used in the turbines of the DOE/SNL SWiFT project.[12] This SWiFT blade was used in this paper.

To generate the geometric profile and composite layup of a wind turbine blade, a fully parametric finite element software was developed using the commercial FE code Abaqus.[13] The most important aspects of creating a finite element model of a wind turbine blade are briefly described below:

1. Aerodynamic geometry of the blade

Wind turbine blades have complex aerodynamic profiles to maximize the potential of wind velocity to generate power. A typical wind turbine rotor consists of several airfoil cross-sections along the length (span) of the blade, as seen in Fig. 1 (Left) for the SWiFT wind turbine rotor. The airfoil coordinates and other necessary blade geometry parameters, e.g., spanwise location, chord length, twist, offset from blade reference axis of the stations were gathered

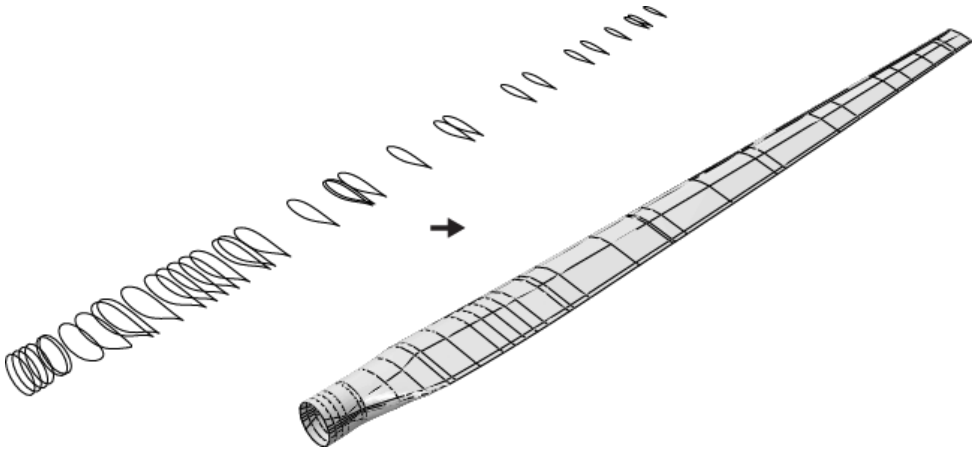

Figure 1. (Left) Airfoil profiles of the Swift wind turbine blade. (Right) Resultant geometric profile of the Swift wind turbine blade.

from the report[8] published by SNL to reproduce the wind turbine blade profile in Abaqus. These airfoil profiles were lofted together to create the geometry of the wind turbine blade. The SWiFT wind turbine blade airfoil profiles and the resultant geometry of the blade can be seen in Fig. 1 (Right). Each station were further divided into an appropriate number of regions with the help of the datum points feature of Abaqus to facilitate the definition of different composite layups.

2. Composite layup definition of the blade

Modern wind turbine blade structures are usually made of fiber-reinforced polymers (FRP), due to their superior strength-to-weight ratio and higher fatigue life compared to metals. The blade of interest for this study is made of glass-fiber reinforced polyester resin. The material properties and the composite layup of the blade are provided in the

Table 1. Elastic properties of the blade materials.

Material	E_{11} (MPa)	E_{22} (MPa)	G_{12} (MPa)	ν_{12}	Density (kg/m^3)	Layer Thickness (mm)
Gelcoat	3440	-	1380	0.3	1230	0.5
M300 Rand-Mat	8880	-	3380	0.3	2212.5	0.2457
T900 (DB600/UD300)	14620	5930	6590	0.486	2212.5	0.7371
NM450	37000	8760	3840	0.3	2212.5	0.36855
PVC Foam	256	-	22	0.3	200	1.0
UD700/M100	33480	8830	3780	0.3	2212.5	0.6552
UD1200	37000	8760	3840	0.3	2212.5	0.9828

previously mentioned report published by SNL. The elastic properties of the blade materials are reported in Table 1. The materials Gelcoat, M300 and PVC Foam in the table are isotropic, while the material names starting with the prefix 'UD' are uniaxial continuous reinforced composites. The T900 material listed in the table is a triaxial composite material.

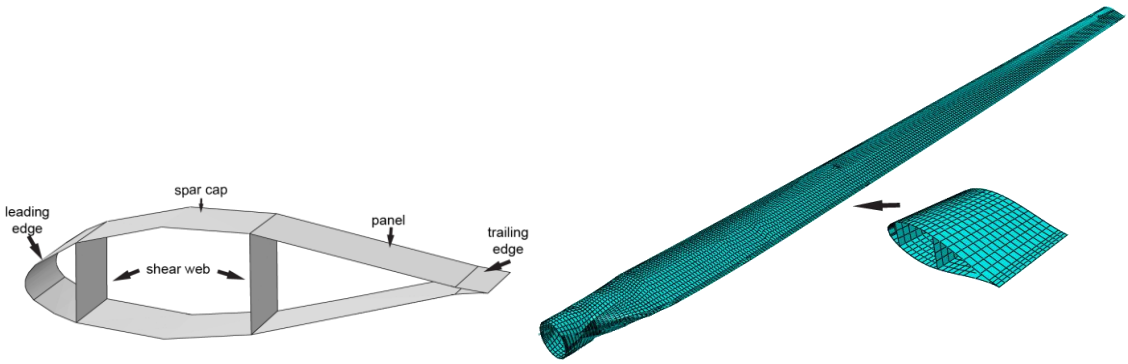

Figure 2. (Left) Schematic of a typical cross-section of the wind turbine blade. (Right) Blade structure meshed with shell elements.

A typical structural architecture of the blade is presented in Fig. 2. The blade is made of three main parts – 1) a high pressure skin, 2) a low pressure skin, and, 3) a box-beam type construction between the HP and LP surface, which is a reinforcing structure of unidirectional composite beams and shear web columns.

The skin of the turbine blade is made of a variety of materials - random material fabric, uniaxial fabric, triaxial fabric, foam core and gelcoat. The *spar cap* region is the reinforced region of the skin located along the box beam. This region is made of thick laminate with primarily unidirectional fibers to carry the flapwise bending loads. The skin regions not adherent to the box beam are referred to as *panels*. While most panels have foam cores, it is not present in the *leading edge* or *trailing edge* regions. *Shear webs* are oriented normal to the spar caps and they consist of a variety of materials including the UD fabric, triaxial fabric and random material fabric. At each station of the blade, composite layup has been defined for spar cap, core panels, leading and trailing edge reinforcements and shear webs.

B. CFD Model to Generate Realistic Load Profile on the Blade

Using the Reynolds-averaged Navier-Stokes (RANS) computational fluid dynamics (CFD) code NSU3D[9, 14], realistic loads were computed on the wind turbine blade. These high-fidelity loads were applied directly in a structural dynamics simulation in the commercial code Abaqus. Coupling of the CFD code with the blade FEA model was performed using an in-house standalone fluid-structure interface module. The aerodynamic forces were measured at each node of the blade from the CFD analysis. Wind loads were calculated for an inflow velocity of 12 m/s with the

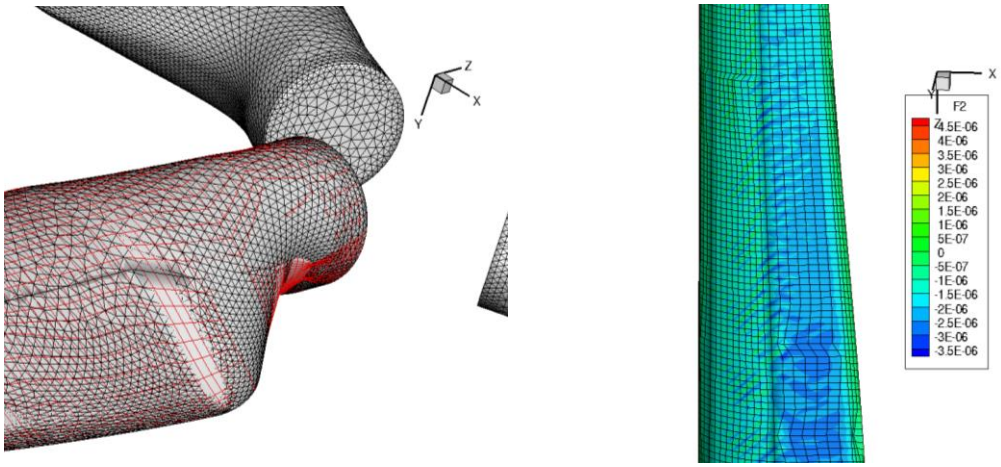

Figure 3. (Left) CFD grid on the Swift wind turbine blade. (Right) Resultant pressure on the nodes of the blade at 12 m/s inflow velocity and 43 rpm of the rotor.

blade rotating at 43 rpm, which is the optimum operating condition for power generation of the SWiFT blade. Figure 3 (Left) presents the CFD mesh on the blade and Fig. 3 (Right) shows the resultant pressure distribution on the nodes of the blade at this operating condition. Since the turbulent regions of the wind field is not being accounted for, the wind loads are constant for a given inflow velocity.

C. Physics-based Composite Fatigue Model

With the exception of nearly perfect axial loading, fatigue failure is primarily a matrix-dominated event for polymer-matrix composites. Fatigue damage initiates with the accumulation of microcracks in the polymer. This microcrack accumulation process is the most rapid during the early stages of fatigue life, and eventually these microcracks coalesce and form a macrocrack which leads to ultimate catastrophic failure of the composite. Therefore, an accurate fatigue prediction for composite materials requires a modeling approach that calculates the microcrack accumulation during each loading cycle.

For the case of a fiber-reinforced polymer (FRP) composite material, the fatigue failure mechanism can be modeled with the kinetic theory of fracture (KTF).[15-19] Since the stresses in the polymer matrix of FRP composites are not the same as the stresses in the composite itself, a methodology for determining matrix stresses from the composite level stresses is required in order to apply KTF to the polymer. The fatigue model used here utilizes the multicontinuum theory (MCT) to extract these polymer matrix stresses from composite stresses.

1. Multiscale approach for linking composite stress with matrix stress

Multicontinuum theory (MCT) provides an efficient approach to extract constituent stress/strain state from the composite stress/strain state. MCT is described amply in the open literature.[20, 21] Since MCT is computationally efficient, very little additional computational time is added to the finite element analysis of the composite structure to extract the constituent stresses. The exact value of volume-average stress in the matrix $\boldsymbol{\sigma}_m$ can be computed from the composite stress state $\boldsymbol{\sigma}_c$ as:

$$\boldsymbol{\sigma}_m = \mathbf{Q}_m \boldsymbol{\sigma}_c - \boldsymbol{\psi}_m \Delta T \tag{1}$$

where,

$$\mathbf{Q}_m = \mathbf{C}_m \left\{ \mathbf{C}_c \left(\varphi_m \mathbf{I} + \varphi_f \mathbf{A} \right) \right\}^{-1}$$

$$\boldsymbol{\psi}_m = \mathbf{C}_m \left\{ \phi_f [(\mathbf{C}_c - \mathbf{C}_f)\left(\varphi_m \mathbf{I} + \varphi_f \mathbf{A} \right)]^{-1} \mathbf{a} + \boldsymbol{\eta}_m - \left(\varphi_m \mathbf{I} + \varphi_f \mathbf{A} \right)^{-1} \boldsymbol{\eta}_c \right\}$$

$$\mathbf{A} = -\frac{\varphi_m}{\varphi_f} \left(\mathbf{C}_c - \mathbf{C}_f \right)^{-1} \left(\mathbf{C}_c - \mathbf{C}_m \right) \tag{2}$$

$$\mathbf{a} = (\mathbf{C}_c \boldsymbol{\eta}_c - \phi_f \mathbf{C}_f \boldsymbol{\eta}_f - \phi_m \mathbf{C}_m \boldsymbol{\eta}_m)$$

In Eqn. (2), $\boldsymbol{C_f}$, $\boldsymbol{C_m}$ and $\boldsymbol{C_c}$ are the reduced stiffness matrices and $\boldsymbol{\eta_f}$, $\boldsymbol{\eta_m}$ and $\boldsymbol{\eta_c}$ are the thermal expansion coefficients for the fiber, matrix and composite, respectively. ϕ_f and ϕ_m represent the matrix and fiber volume fraction, respectively.

2. Kinetic Theory of Fracture (KTF)

The kinetic theory of fracture (KTF), which describes bond breaking as a thermally activated process, captures the relevant physics of polymer matrix fatigue.[15-18, 22] KTF was developed more than fifty years ago independently by Zhurkov[19] and Coleman.[15] The basic form of KTF is given by:

$$K = \frac{kT}{h} \exp\left(\frac{-U}{kT} \right) \tag{3}$$

where, U is the energy barrier, k is the Boltzmann's constant, T is the absolute temperature and h is the Planck's constant.

The basic equation of KTF can be modified to give the bond breaking rate of the thermally activated process as:

$$K_b = \frac{kT}{h}\exp\left(-\frac{U-\gamma\sigma(t)}{kT}\right) \tag{4}$$

Equation (4) is the basic equation for modeling composite fatigue, as it gives the rate of bond breaking/microcracking under the effect of constant stress and temperature.

Hansen and Baker-Jarvis[23] used KTF to investigate the relationship between the microcrack accumulation in the matrix and the macroscopic failure of the composite material, thus linking the microscopic physics with the macroscopic behavior. They introduced a damage parameter, *n*, to link the microcrack accumulation with macroscopic damage. The damage parameter *n* represents the fraction of microcrack density accumulated with the microcrack density at failure; therefore the damage variable is zero initially and unity at failure. Here we follow the work of Fertig and Kenik[6, 7] to write the differential equation describing the evolution of the damage parameter.

$$\begin{aligned} \frac{dn}{dt} &= (n_0 - n)^{\lambda} K_b \\ n(0) &= 0 \end{aligned} \tag{5}$$

Here λ is a damage accumulation exponent, K_b is calculated from eq. (4) and n_0 is an equilibrium parameter that is determined by enforcing the following condition:

$$\int_0^1 \frac{dn}{(n_0 - n)^{\lambda}} = 1 \tag{6}$$

Assuming a constant nominal temperature, Eqs. (5) and (4) can be combined to yield the starting equation for determining the fatigue life of a polymer.

$$\frac{dn}{dt} = (n_0 - n)^{\lambda}\frac{kT}{h}\exp\left(-\frac{U-\gamma\sigma(t)}{kT}\right) \tag{7}$$

Integrating Eq. (7) we can compute the evolution of the damage parameter with time.

3. Determining the effective stress in the matrix

Using eq. (1) we can compute the volume-average matrix stress tensor. However, a scalar measure of the matrix stress state is required for use in KTF. It has been shown in the literature that fatigue stress normalized by the static failure strength is an appropriate measure for predicting the fatigue life.[24, 25] Therefore, to determine the effective stress in the matrix, we utilize the functional form of the static failure criteria.

The off-axis failure mode is our first mode of interest. For this particular failure mode, it has been observed in the literature that fatigue failure in unidirectional composite occurs frequently due to cracking parallel to fibers[26, 27]. Consequently, it is expected that a substantial role in fatigue is played by tensile forces perpendicular to the fiber direction as well as the shear stresses on these planes. Taking the axial direction of the fiber as the 1-direction, Fertig proposed an *in situ* matrix failure criterion[5] in the form of transversely isotropic invariants of the matrix stress tensor that takes the following form:

$$B_t\{I_t\}^2 + \frac{1}{1+\frac{\beta}{\tau_0}\{-I_h\}}[B_{s1}I_{s1} + B_{s2}I_{s2}] = 1 \tag{8}$$

where,

$$\begin{aligned} I_t &= \frac{\sigma_{22}^m + \sigma_{33}^m + \sqrt{(\sigma_{22}^m + \sigma_{33}^m)^2 - 4(\sigma_{22}^m\sigma_{33}^m + (\sigma_{23}^m)^2)}}{1+\frac{\beta}{\tau_0}\{-I_h\}} \\ I_{s1} &= (\sigma_{12}^m)^2 + (\sigma_{13}^m)^2 \end{aligned} \tag{9}$$

$$I_{s2} = \frac{1}{4}(\sigma_{22}^m - \sigma_{33}^m)^2 + (\sigma_{23}^m)^2$$

$$I_h = \sigma_{22}^m + \sigma_{33}^m$$

The {} denote the Macaulay brackets such that the enclosed term would take the value zero if the encompassed quantity is negative, the σ_{ij}^m values correspond to the matrix stress tensor components. We can determine the value of B_i from three lamina level static failure tests: transverse tension, transverse compression, and in-plane shear, all of which involve failure of the matrix constituent. We can obtain an off-axis effective stress by dividing eq. (9) by B_{s1} and arrive at:

$$\sigma_{eff}^{off-axis} = \sqrt{A_t\{I_{m,t}\}^2 + \sigma^2{}_{m,12} + \sigma^2{}_{m,13} + A_s(\frac{1}{4}(\sigma_{m,22} - \sigma_{m,33})^2 + \sigma_{m,23}^2)} \quad (10)$$

where the coefficients A_t and A_s can be readily obtained from the static failure coefficients as:

$$A_t = \frac{B_t}{B_{s1}}, \qquad A_s = \frac{B_{s2}}{B_{s1}} \quad (11)$$

D. Integration with Finite Element Analysis

The process described in sections II.A-II.C has been implemented in the commercially distributed composite analysis software Helius PFA[28] which works as an add-on for commercial finite element codes such as Abaqus.[13] Helius PFA implements the fatigue failure methodology described in this paper using the User Defined Material (UMAT) feature of Abaqus. The workflow for implementation of the fatigue methodology in Abaqus using Helius PFA is as follows. First, a composite material is calibrated for use with the physics-based methodology described above. This involves calculating the *in-situ* properties of the composite and also the parameters required for KTF calculations – U and γ. The calibration of these parameters requires the knowledge of the material elastic properties, static strengths and two lamina-level fatigue characterization curves (S-N curves, one on-axis and one off-axis). After the materials are characterized, a finite element model is created for the problem with a reference load, P_{ref}, which is typically the largest load in the load history. The input file for the analysis is then created with the required changes made to incorporate the usage of Helius PFA. As the input file for the problem is executed, the composite stresses calculated by the finite element code are sent as an input to Helius PFA where the fatigue model is implemented. The damage state of the matrix, the number of cycles to failure and other necessary information are written in the output file.

III. Simulation and Results

In this section we present the analysis results for our test blade. All the analyses have been performed in the commercial finite element code Abaqus, using the software Helius PFA as an UMAT that implements the physics-based fatigue life model. As a test case, the wind turbine blade was taken to be operating at 43 rpm and with inflow velocity of wind at 12 m/s – condition for maximum torque generation of the blade.[8] The finite element model of the wind turbine blade was created with reduced integration shell elements (S4R and S3R in Abaqus) with 0.05m element size. All six degrees of freedom at the root end of the blade were constrained.

A. Static Analysis of the Wind Turbine Blade

1. Mass and Modal Frequency comparison

The results of mass and modal frequency comparison between the SWiFT wind turbine model created at the University of Wyoming and the one created by the Sandia National Labs have been presented in Table 2. Since the blade composite layup data was not available with all the details, it was not possible to accurately match the wind turbine model with the SNL model. Table 2 shows that the mass

Table 2. Mass and Free-Free Modal Frequency comparison between University of Wyoming (UW) model and Sandia National Labs (SNL) model.

	SNL Model	UW model	% of Error
Mass (Kg)	596.9	542.71	- 9.0786%
1st Flap (Hz)	4.816	6.3955	32.7969%
1st Edge (Hz)	10.09	10.721	6.2537%
2nd Flap (Hz)	12.56	15.311	21.9029%

properties do not match for the blades, which eventually creates the mismatch between the modal frequencies. However, for the purpose of this paper it was deemed that the model very closely replicated a realistic wind turbine blade and should provide valuable insight about its fatigue failure process.

2. Loads on the wind turbine blade

Three major sources of loading experienced by a wind turbine rotor during operation are: 1) gravitational loading, 2) inertial loading, and 3) aerodynamic loading.

The gravitational loading causes a sinusoidal varying loading pattern on the rotating blade. The typical lifetime for a wind turbine blade is considered to be 20 years, and during this lifetime, it goes through 10^8 – 10^9 cycles. Therefore, gravitational loading plays a major role to create the cyclic loading on a wind turbine blade.

The aerodynamic forces are caused by the wind flow past the structure. In literature, the wind pressure and the wind flow-turbine interaction is simulated with various simplifying assumptions. In our analysis, time dependent wind load was generated on the wind turbine rotor using the CFD code NSU3D via an in house fluid-structure interface module described in details in part II.

The inertial loading is caused by the centrifugal forces acting on the blade during rotation.

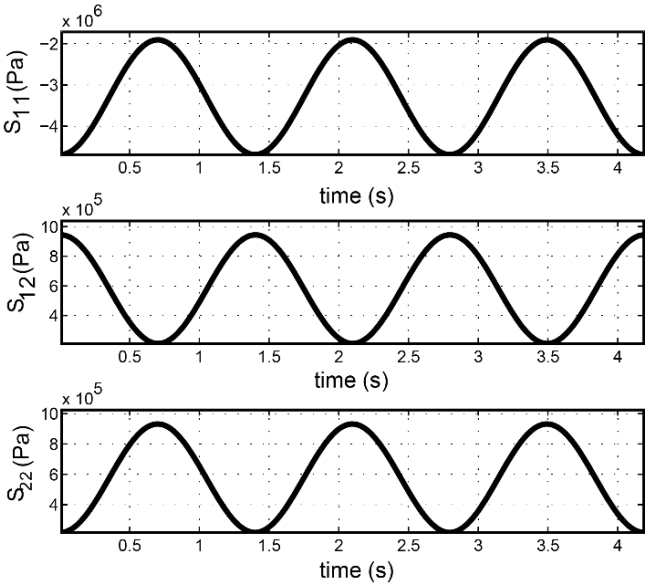

Figure 3. Time variation of stress components of a section point.

A combination of all the above mentioned forces - aerodynamic, centrifugal and gravitational loading have been applied on the test blade to simulate the typical working condition of a wind turbine rotor. The resultant stress-time series is presented in Fig. 3. The cyclic nature of the load is evident from the figure.

B. Fatigue Simulation of the wind turbine blade using Helius PFA

A wind turbine blade works under multi-axial loading, which causes non-linear damage accumulation in the blade. However, the common fatigue analysis procedures of wind turbine blade assume linear damage accumulation rules[29, 30]. In a recent publication, Hu et al.[31] used Miner's sum (a linear damage model) to calculate damage accumulation in a wind turbine blade. The fatigue damage methodology used in this paper does not use such linear approximations (section II.B) and is capable of working with a multi-axial complex stress-state which is typical of a wind turbine blade. Moreover, Fertig et al. [6] has shown that this methodology can be used to predict the fatigue behavior of angle-ply laminate based on lamina level characterization.

The fatigue methodology requires in-situ properties of the constituents, static strength of the laminae and two fatigue characterization curves. Even though the report by SNL provides a great deal of information about the SWiFT wind turbine blade, unfortunately it does not provide any lamina strength or fatigue S-N data that is required by our methodology to fully characterize the laminate. Hence we adopted the strength properties of material S2_Glass_Epoxy2 from the material library of Helius PFA, along with the in-situ properties of the glass fiber and

Table 3. In-situ properties and lamina strength properties used in the fatigue model collected from Helius PFA material manager.

	E_{11}	E_{22}	G_{12}	ν_{12}	ν_{23}	$+S_{11}$	$-S_{22}$	S_{12}
Fiber (glass)	8.000E+10	8.000E+10	3.333E+10	0.200	0.20			
Matrix (thermoset epoxy)	3.500E+09	3.500E+09	1.296E+09	0.350	0.35			
composite						1.70E+09	-1.80E+08	7.20E+07

thermosetting polymer matrix. These properties have been presented in Table 3. As noted earlier, two fatigue curves are required to characterize the fatigue behavior of a lamina in Helius – one longitudinal fatigue curve and another off-axis fatigue curve. The S-N data to characterize the laminas of the SWiFT blade were taken from the work by Hashin and Rotem[3] for a E-glass/epoxy composite. Table 4 reports the data.

Table 4. Fatigue S-N data for the blade materials. Properties of E-glass/epoxy composite found in literature.

Stress (Pa)	N	f (Hz)	R	Angle of Loading
9.344E+08	2.08E+04	18.8	0.1	0
9.045E+08	3.44E+04	18.8	0.1	0
8.802E+08	4.79E+04	18.8	0.1	0
8.447E+08	6.40E+04	18.8	0.1	0
8.148E+08	8.00E+04	18.8	0.1	0
2.956E+07	6.20E+02	19	0.1	60
2.805E+07	2.69E+03	19	0.1	60
2.635E+07	8.99E+03	19	0.1	60
2.484E+07	6.23E+04	19	0.1	60
2.352E+07	1.54E+05	19	0.1	60

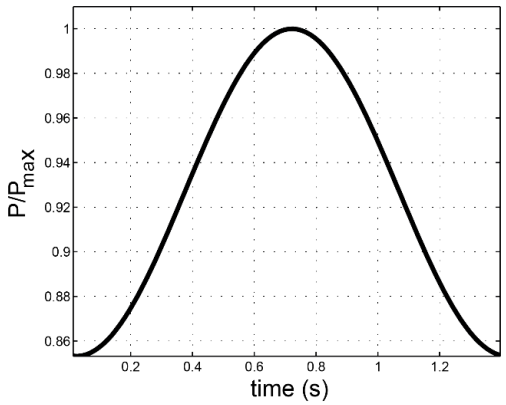

Figure 4. P/P_max variation during one full revolution of the wind turbine blade rotating at 43 rpm.

A static analysis of the test blade was performed as a prequel to the fatigue simulation to determine the cyclic loading on the blade during one complete cycle. The effective stress state of the matrix (called SDV2 in Helius, a solution-dependent MCT state variable) has been used to generate the fatigue loading cycle on the blade. The region with the maximum value of SDV2 has been chosen to define the cyclic loading on the blade, since high stress concentration areas are the likely regions for the initiation of failure. Figure 4 shows the fatigue loading cycle used for progressive fatigue analysis of the blade.

The fatigue simulation of the SWiFT blade was performed with the maximum value of the static load applied on the blade, along with the load variation shown in Fig. 4 used to define the fatigue loading cycle. Since Helius can be

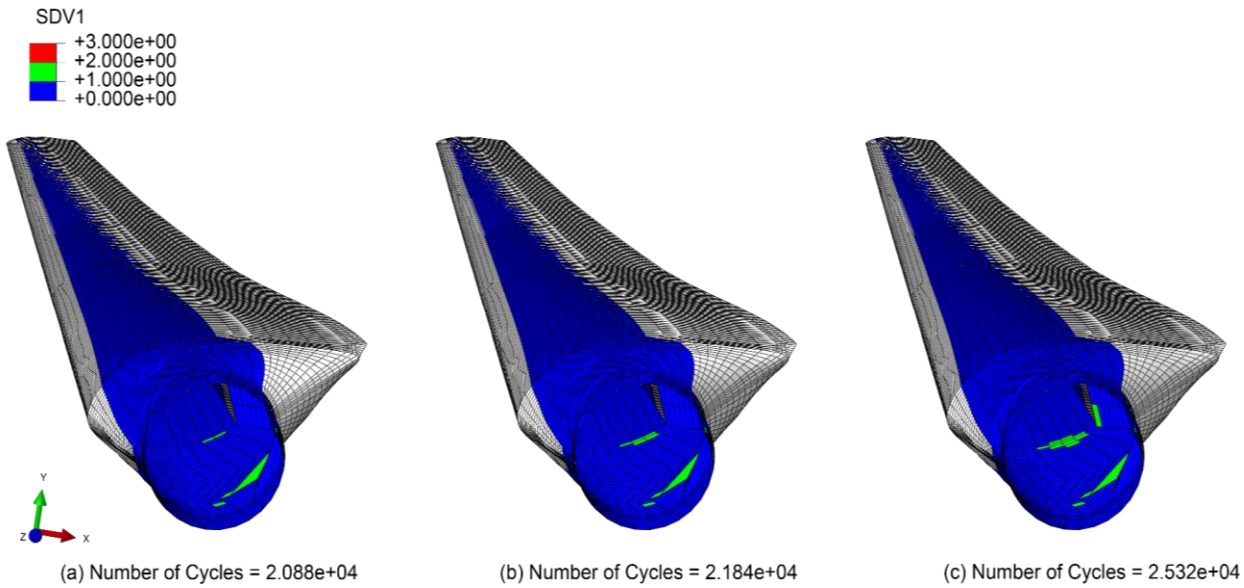

Figure 5. Initiation and propagation of matrix failure in the Swift wind turbine blade in as indicated by the failure index.

applied to unidirectional and woven composites, we have performed our analysis on the plys of the unidirectional composite laminates of the SWiFT blade. Therefore, the isotropic materials and the T900 triaxial material of Table 1 were not included in the fatigue analysis.

The results from this analysis are presented in Fig. 5. The damage state is represented by SDV1 and the indices correspond to: 1 = no failure (blue), 2 = matrix failure (green) and 3 = matrix and fiber failure (red). The maximum fatigue damage of section points through the laminate thickness is used to represent the damage for each element. As can be seen from the Fig. 5, the initiation of matrix failure occurs near the root region, the high stress concentration region of the blade. The matrix failure shown here is the first ply failure and does not indicate that the matrix of the whole laminate has failed. This indicates the capability of prediction of fatigue critical areas of the blade. We can also identify the specific ply(s) in the composite laminate where matrix damage initiates and subsequently propagates with increasing load cycles. The maximum values of matrix damage occurred in ply 26 of the spar cap composite laminates containing the *UD1200* unidirectional ply.

IV. Conclusion

We have outlined a comprehensive methodology for investigating fatigue life of a realistic wind turbine blade using a physics-based methodology in conjunction with the realistic aerodynamic loads. A composite wind turbine blade was designed in the finite element code Abaqus using data provided by Sandia National Labs. Details on creating the blade model and the blade properties have been documented in this paper. High-fidelity aerodynamic loads were generated on the blade using the CFD code NSU3D for a test case of 12 m/s wind velocity. Gravity and centrifugal forces were also defined on the blade, creating a multi-axial variable amplitude loading condition on the blade. A physics-based fatigue methodology was used to evaluate the fatigue life of the wind turbine blade under this complex stress-state. The obtained results identified the fatigue-critical areas of the blade, showed the initiation and propagation of damage and also quantified the amount of fatigue damage accumulated in the composite laminates. Since this fatigue methodology is computationally efficient and requires little material characterization data, it has the potential to be a powerful tool for design of fatigue critical composite structures.

Acknowledgments

Funding for this work is gratefully acknowledged from the University of Wyoming's College of Engineering and Applied Sciences Energy Graduate Assistantship.

References

1. Krohn, S., P.-E. Morthorst, and S. Awerbuch, *The Economics of Wind Energy: A report by the European Wind Energy Association.* European Wind Energy Association, Brussels. Available online at: http://www. ewea. org/fileadmin/ewea_documents/documents/00_POLICY_document/Econom ics_of_Wind_Energ y__March_2009_. pdf, 2009.
2. Wood, K., *Blade repair: Closing the maintenance gap.* Composites Technology, 2011.
3. Hashin, Z. and A. Rotem, *A fatigue failure criterion for fiber reinforced materials.* Journal of composite materials, 1973. **7**(4): p. 448-464.
4. Talreja, R. *Fatigue of composite materials: damage mechanisms and fatigue-life diagrams*. in *Proceedings of the Royal Society of London A: Mathematical, Physical and Engineering Sciences*. 1981. The Royal Society.
5. Fertig, R. *Bridging the gap between physics and large-scale structural analysis: a novel method for fatigue life prediction of composites*. in *Proceedings of the SAMPE Fall Technical Conference*. 2009.
6. Fertig III, R.S. and D.J. Kenik, *Predicting Composite Fatigue Life Using Constituent-Level Physics.* 2011.
7. Fertig, R. and D. Kenik. *Physics-based fatigue life prediction of composite structures*. in *NAFEMS World Congress 2011*. 2011.
8. Resor, B.R. and B. LeBlanc, *An Aeroelastic Reference Model for the SWIFT Turbines*. 2014, Sandia National Laboratories.
9. Mavriplis, D., *NSU3D (Version 3.3)–A CFD Package for External Aerodynamics using an Unstructured Navier-Stokes Multigrid Solver.* NSU3D User Manual, 2000.
10. Griffith, D.T., B.R. Resor, and T.D. Ashwill. *Challenges and opportunities in large offshore rotor development: Sandia 100-meter blade research*. in *AWEA WINDPOWER 2012 Conference and Exhibition*. 2012.
11. Griffith, D.T. and T.D. Ashwill, *The Sandia 100-meter all-glass baseline wind turbine blade: SNL100-00.* Sandia National Laboratories, Albuquerque, Report No. SAND2011-3779, 2011.
12. *The Scaled Wind Farm Technology (SWiFT)*
13. *Abaqus, Version 6.14-1, product of Dassault Systèmes Simulia Corp., 2014, Providence, RI, USA.*

14. Mavriplis, D. and M. Long, *NSU3D Results for the Fourth AIAA Drag Prediction Workshop.* Journal of Aircraft, 2014. **51**(4): p. 1161-1171.
15. Coleman, B.D., *Time dependence of mechanical breakdown phenomena.* Journal of Applied Physics, 1956. **27**(8): p. 862-866.
16. Regel', V., et al., *Polymer breakdown and fatigue.* Mechanics of Composite Materials, 1972. **8**(4): p. 516-527.
17. Tamuzh, V., *Fracture and fatigue of polymers and composites (survey).* Polymer Mechanics, 1977. **13**(3): p. 392-408.
18. Sauer, J. and G. Richardson, *Fatigue of polymers.* International journal of fracture, 1980. **16**(6): p. 499-532.
19. Zhurkov, S.N., *KINETIC CONCEPT OF THE STRENGTH OF SOLIDS.* International Journal of Fracture, 1984. **26**(4): p. 295-307.
20. Garnich, M.R. and A.C. Hansen, *A multicontinuum approach to structural analysis of linear viscoelastic composite materials.* Journal of Applied Mechanics-Transactions of the Asme, 1997. **64**(4): p. 795-803.
21. Garnich, M.R. and A.C. Hansen, *A multicontinuum theory for thermal-elastic finite element analysis of composite materials.* Journal of Composite Materials, 1997. **31**(1): p. 71-86.
22. Kireenko, O. and A. Leksovskii, *VR Regel'," Polymer fractography and fracture kinetics. 3.* Fractographic method of estimating the local heating at the ends of cracks in cyclically loaded polymers," Mekh. Polim, 1971(5): p. 869-874.
23. Hansen, A.C. and J. Baker-Jarvis, *A rate dependent kinetic theory of fracture for polymers.* International Journal of Fracture, 1990. **44**(3): p. 221-231.
24. Awerbuch, J. and H. Hahn, *Off-axis fatigue of graphite/epoxy composite.* Fatigue of fibrous composite materials, ASTM STP, 1981. **723**: p. 243-73.
25. Kawai, M., et al., *Off-axis fatigue behavior of unidirectional carbon fiber-reinforced composites at room and high temperatures.* Journal of Composite Materials, 2001. **35**(7): p. 545-576.
26. Kawai, M. and T. Taniguchi, *Off-axis fatigue behavior of plain weave carbon/epoxy fabric laminates at room and high temperatures and its mechanical modeling.* Composites Part A: Applied Science and Manufacturing, 2006. **37**(2): p. 243-256.
27. Petermann, J. and A. Plumtree, *A unified fatigue failure criterion for unidirectional laminates.* Composites Part A: Applied Science and Manufacturing, 2001. **32**(1): p. 107-118.
28. *Autodesk Helius PFA 2016*
29. Standard, I., *61400-1 3rd Edition, 2005.* Wind turbine generator systems-Part. **1**.
30. Germanischer, L., *Guideline for the Certification of Wind Turbines Edition 2010 [G]*. 2010, Germany.
31. Hu, W., et al., *Integrating variable wind load, aerodynamic, and structural analyses towards accurate fatigue life prediction in composite wind turbine blades.* Structural and Multidisciplinary Optimization, 2015: p. 1-20.